Proceedings World Geothermal Congress 2020+1
Reykjavik, Iceland, April - October 2021

Comparative Analysis of Energy Extraction Systems for High Temperature, High Pressure Geothermal Steam Considering Silica Precipitation

Silje Bordvik, Erling Næss

NTNU, Kolbjørn Hejes vei 1D, 7034 Trondheim, Norway

silje.bordvik@ntnu.no

erling.nass@ntnu.no

Keywords: geothermal power systems, supercritical water, silica, precipitation, scaling, geomagma, nanoparticle deposition

ABSTRACT

This paper presents the results from an analytical comparison of energy extraction systems from high temperature, high-pressure geothermal steam when taking into consideration dissolved silica according to quartz equilibrium in the reservoir. The comparisons include backpressure turbines, steam reheat, binary and hybrid solutions, conventional steam turbines and combinations of these. Experimental and computational research from the last four decades are summarized to address where and how amorphous silica may become problematic in the systems considered. A combination of thermodynamic calculations of super-saturation index, models for kinetics of particle formation and -growth, and computational fluid dynamic modelling of suspended particle deposition in nanoscales is used for the evaluations. The fluid in consideration is supercritical steam from a 4-5 km deep well with a nearby magmatic heat source, giving wellhead temperatures ranging between 400 and 550 °C at 350 bar pressure. The reservoir fluid is supercritical, while the conditions at wellhead may be superheated steam depending on the pressure loss during production. The fluid composition is estimated based on expected composition of IDDP2 well drilled in Reykjanes, Iceland. The analysis show that the dissolved silica content is high enough to necessitate some form of purification before entering a conventional turbine. The equipment upstream the scrubber needs to be robust with regard to silica precipitation/scaling and the pressure reduction and downstream equipment optimized to ensure as little energy loss as possible with as little downstream silica contamination as possible. The alternatives presented are rated with regard to power output, energy utilization efficiency and their robustness against silica scaling.

1. INTRODUCTION

Solid precipitation cause challenges in many geothermal systems around the world today. In high temperature application silica scaling is the most problematic (DiPippo 2016) and silica precipitation is therefore the main focus of these evaluation cases. Significant carryover of volatile $Si(OH)_4$ from water to steam has been observed at higher pressures (Bahadori and Vuthaluru 2009). Silica in steam turbines deposit on turbine blades and nozzles, distorting the original shape of the blade, cause roughness, uneven flow and flow resistance. All contribute to increased losses in the turbine and even uneven distribution of load, leading to rotor imbalance and unhealthy vibrations. (Zarrouka, Woodhursta et al. 2014) analyzed the consequence of monomeric silica deposition inside heat exchangers in the Wairakei binary plant in New Zealand and found that overall performance was reduced due to increased pressure losses. Clogging of reinjection wells is another common challenge that has received attention because well intervention and recompletion is expensive. A conventional well producing hot liquid water at 230 °C and 50 bar at wellhead could have a silica concentration of 600-900 mg/kg on average. The liquid will be flashed at a lower pressure and equilibrium concentration of silica in the steam phase is very low at lower pressures, so little carry over is expected even though the overall concentration is high. For the cases we are looking at it is assumed that the wellhead conditions will be in the supercritical steam region (500°C and 350 bar). Equilibrium concentration of silica in pure water at this pressure and temperature is approximately 190 mg/kg (Fournier and Potter 1982a) and this concentration is assumed as a base case. The equilibrium concentration of silica is so low that the solution is undersaturated if cooled to liquid state, but a very rapid change in supersaturation occurs if the supercritical steam is depressurized into the superheated steam region or the two-phase region. The rate of change in supersaturation when depressurizing supercritical steam differ from the changes observed when cooling water or increasing concentration in liquid water, as would be the case when flashing of steam. Supersaturation index is defined as actual concentration over the equilibrium concentration. The kinetics of nucleation, growth and final morphology of the silica precipitate will also differ greatly, affecting population balance and characteristics. The hydrodynamic behavior of the resulting colloids in the fluid flow will depend on the particle characteristics as well as the flow field.

2. SILICA PRECIPITATION FROM SUPERCRITICAL STEAM

2.1 Physical and chemical properties of supercritical geothermal steam

Liquid water at ambient conditions is a powerful solvent for many minerals, especially polar substances and hydrogen bond forming minerals. This quality as a solvent is largely attributed to the hydrogen bond structure between water molecules and the high dielectric constant and viscosity it leads to (Palmer, Fernández-Prini et al. 2004) (Churakov 2001). The hydrogen bond is a particular type of intermolecular interaction which can be observed between hydrogen and an electronegative atom of a different molecule. The hydrogen atom is partly charged because the electron density around the atom can be deformed. When waters enters the steam phase, the structure of hydrogen bonds dissolve and the electrolytic power is lost. Steam prefer to mix with nonpolar gases and some organic compounds. Already at 150°C, increase in thermal motion disrupt the tetrahedral orientation of the water molecules. In the supercritical phase, that is above the critical point of 221 bar and 374°C, the degree of hydrogen bonding in the water vary with temperature and pressure. The liquid like structure on the left side of the phase diagram will have a higher degree of hydrogen bonding, but at high pressures hydrogen bonding has been shown to persist in clusters up to high temperatures. Proton NMR data

indicate that the degree of hydrogen bonding at a temperature of 500°C and 430 bar is 13% (Palmer, Fernández-Prini et al. 2004). The solubility of molecular substances or ionic species depend on their ability to disrupt the hydrogen bond network. When hydrogen bond network is dissolved in the supercritical state, the mineral formation and dissolution is affected. The chemical diffusivity increases while the acidity is enhanced more than can be attributed to the rise in temperature (Palmer, Fernández-Prini et al. 2004). The switchover from a polar to a non-polar solvent also result in an increase in stability of neutral polymerized species over solvated ions, resulting in enhanced solubility of silicate minerals (Hack, Thompson et al. 2007).

2.2 Silica solubility and precipitation kinetics

For temperatures above 185°C the silica content in the geothermal fluid is normally determined from the equilibrium value of quartz. Above this temperature the reaction rates are so high that metastable silica phases (like glass, opal and silica gels) are unlikely to persist. A correlation was developed by (Fournier and Potter 1982b) giving accurate data for equilibrium concentrations of quartz in the supercritical region. Dissolution and precipitation of silica follow the reaction rate $SiO_2 + 2H_2O = H_4SiO_4$. In pure water, H_4SiO_4 was shown by (Brady 1953) and (Jacobson, Opila et al. 2005) to be the dominant carrier species of Silica also for the steam phase. From multicomponent steam mixtures such as observed volcanic fumaroles, other species, like silica combined with fluoride (SiF_4) and chloride ($SiCl_3$) has been observed in significant amounts (Churakov 2001) (Masanori, Yoichi Shimoike et al. 2014). It is interesting to note that hydrolysis of gaseous SiF_4 or $SiCl_4$ at the gas-liquid interface and simultaneous polymerization of the silicic acid in water has been shown, at lower temperatures and pressures, to produce “opaque” scales of silica behaving like films of silica gel formed at the surface. The powder generated is characterized as “fluffy” with a bulk density as low as 0,025 g/cm3 (Iler 1979).

Due to the relatively slow reaction rates of quartz and cristoballite, these forms of silica have rarely been observed in geothermal systems. Precipitation potential is determined by the equilibrium concentration of amorphous silica, which is higher, but with a reaction time fast enough to cause precipitation in the system. A thermodynamic framework for calculating amorphous silica concentrations in the supercritical region has been proposed by (Plyasunov 2012) and (Karásek, Šťavíková et al. 2013). Also a range of experimental data on amorphous silica solubility is available from (Morey and Hesselgesser 1951), (Heitmann 1964) and (Kennedy 1944) among others. As for the quartz form, amorphous silica in the superheated and supercritical steam regions can be correlated with specific volume (Fournier and Rowe 1977).

The precipitation in this context is defined as solid material derived from the geofluid. There are two different mechanisms involved in the formation of silica precipitate in geothermal industry; monomeric silica deposition by condensation and chemisorption on a surface and bulk polymerization and formation of nanocolloids that are carried with the fluid. Monomeric deposition has been shown to be problematic in heat exchanger systems, forming a hard scale that resembles vitreous silica (Zarrouka, Woodhursta et al. 2014). The latter forms a dense porous scale when settled onto a surface and is often associated with much higher scaling rates (Brown 2011). It is the dominant form of scale from supercritical geothermal steam where changes in supersaturation are rapid. In pure water-silica solutions the surface of the silica particle is terminated either with siloxane links (Si-O-Si), as in the bulk, or hydroxyls (Si-OH). The latter is the result of incomplete condensation during the polymerization process. Hydrous silica is characterized by high number of hydroxyls at the surface, which stabilizes the colloid (J. Nestor 2016).

The precipitation process, as opposed to crystallization, is characterized by relatively sparingly soluble substances in high supersaturation leading to rapid solidification. The rapid increase in supersaturation cause a high nucleation rate leading to a high number of primary nuclei formed. Due to a relatively slow monomeric growth rate, agglomeration is favored and hydrodynamics play an important role. The monomeric growth rate is still important as it determines the rate of cementation of agglomerate bridges and resulting nanostructure of the evolving particle.

Due to the extensive industrial use of silica (some examples include xerogel, aerogel and Stöber particles), there is a fair amount of research on silica particle generation. According to the LaMer model the nucleation is homogenous by monomeric addition and relatively fast. As the system moves further towards equilibrium the particles will either grow by Ostwald ripening (Lewis, Seckler et al. 2015), in this case limited by condensation of monomers on the surface of the particles, or by agglomeration. In the aggregative growth model nucleation and aggregation occur simultaneously, resulting in a gel network instead of spherical particles as illustrated in Figure 1(Brinker and Scherer 2013). Interaction forces between particles determine degree of agglomeration. Factors that may influence are particle surface charge, ionic strength of water, pH, silica-water surface tension, concentration and flow characteristics. The aggregation model where the continuous nucleation is rate limiting has been shown to better predict growth of silica particles at various pH.

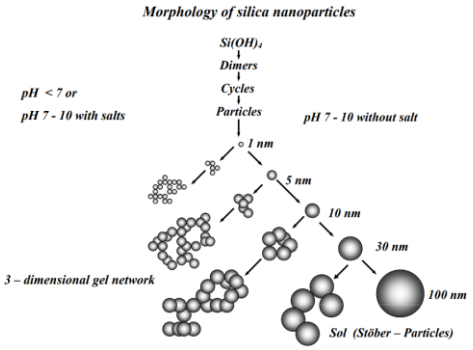

Figure 1: Growth of silica particles (Brinker and Scherer 2013)

The following has been found to be true for silica particle growth (Iler 1979); At pH above 2 the polymerization rate is proportional to the number of OH- ions. At low pH particle growth due to Ostwald Ripening becomes negligible after the particles reach a size of 2-4 nm. At pH values below 6 the particles are also less stable and agglomerate. Presence of salt (above 0,2-0,3 equivalent per liter (N)) leads to further destabilization and gelification. In the early stages of polymerization, ring structures like cyclic tetramers, are formed by the tendency to form maximum siloxane bonds and a minimum of uncondensed SiOH groups. The presence of hydrofluoride has shown to increase polymerization. As little as 1 ppm has a marked effect at low pH. At low concentration of silica, as would be the case for this geothermal steam, the monomers are converted to discrete particles before they begin to agglomerate. Coagulants such as metal cations also lead to precipitation rather than gelling. The result may be nanocolloids in chain like aggregates of low density rather than discrete spherical particles.

Assuming a starting point with a nuclei number density of 10^{17} per kg of fluid, and a nucleus size of 2,5 nm (corresponding to an excess concentration of 200 mg/kg and a silica density of 2196 kg/m3), calculations with the Smoluchowski equation (Lewis, Seckler et al. 2015),(Smoluchowski 19117) for agglomeration kernels given in equation (1) to (4) show that the Brownian motion dominates the agglomeration by a factor of 10^{12}. Growth is slow until the size reaches a certain level where turbulence becomes influential. From there growth is accelerated exponentially. In these equations β is the agglomeration kernels for Brownian motion: size dependent, Brownian motion: process dependent, turbulent shear: process dependent and turbulent shear: size dependent respectively. The kernel β is the product of the size dependent (1) and size independent (0) kernels given in m^3/s. L_i and L_j are characteristic lengths, in this case the particle diameter of two approaching particles. ε, μ, ν, T and k are turbulent diffusivity, dynamic viscosity, kinematic viscosity, temperature and the Boltzman constant respectively.

$$\beta_{1\_BM} = (L_i + L_j)(\frac{1}{L_i} + \frac{1}{L_j}) \tag{1}$$

$$\beta_{0\_BM} = \frac{2kT}{3\mu} \tag{2}$$

$$\beta_{0\_TS} = \sqrt{\frac{\varepsilon}{\nu}} \tag{3}$$

$$\beta_{1\_TS} = (L_i + L_j)^3 \tag{4}$$

The collision efficiency in this example is assumed high (0,9). The surface of a silica particle or polymer is negatively charged, giving rise to electrostatic repulsive force between two particles. The degree of surface charge will depend on pH, ionic strength, absorption of metal cations on the surface and degree of hydration on the surface of the particle. When the particles come close enough the van der Waals forces outweigh the repulsive potential and keep the particles locked together until they are cemented by monomeric growth. Some particles moving towards each other will bounce off due to the repulsive forces and not all collision will lead to attachment. The range of the repulsive force between two particles depend on the Debye-Hückel reciprocal length. As the dielectric constant in the steam phase is very low even at elevated pressures (approximately 2 (Brunner 2014)), the extent of the repulsive force will be lower than for liquid water. The point of zero charge for silica is at pH 2. Generally, it is assumed that at pH below 7 the repulsive force between the 2,5 nm particles is very low. The repulsive force will increase as the particle size increase reducing the collision efficiency. For silica particles in water a spherical gel layer theory has been proposed. The effect of a surface gel layer increases the stability of smaller particles as opposed to standard DLVO theory where stability increase with particle size (Allison 2004).

The particles in the calculation example are not expected to grow significantly within the first minute. The precipitated amorphous silica thus consist of extremely small particles and slightly larger porous aggregates. The surface remains hydrated with SiOH groups, so does the pore surface within the agglomerated particles unless fully cemented. The microstructure and the porosity of the aggregates will affect the electrostatic potential. Even large particles, may have a large internal surface hydrated with SiOH groups due to porosity that increase their stability. The extent of surface hydration will be somewhat lower in supercritical steam than in liquid water, but even humidity in air is enough to hydrate the surface of silica particles to some extent (Papirer 2000).

The deposition on a silica-covered surface is affected by the same electrostatic potential as described for collision between two particles. The deposition of particles on a surface can be calculated using fluid dynamic simulations. Models for particles in gas have been used to simulate silica particle in steam considering the effect of Brownian diffusion, turbulent diffusion, turbophoresis, Saffman lift force, drag force and thermophoresis on silica particle motion (Chauhan, Gudjonsdottir et al. 2018). Theoretically, most of the silica particles should remain in the steam if looking at a short time span. Testing performed on depressurized steam from IDDP1, however, showed deposition rates in piping that were as high as 0,02 mm/hour (Karlsdottir, Ragnarsdottir et al. 2014). Hydrodynamic effects were observed during the erosion-corrosion testing of IDDP1. Hydrodynamic effects of silica scaling in liquid water has also been observed by (Brown and Dunstall 2000) and (Kokhanenko 2014). Detailed modelling of turbulence in the boundary layer is important to predict the deposition of silica from highly supersaturated solutions of geothermal steam.

3. ENERGY EFFICIENCY COMPARISON FOR UTILIZING SUPERHEATED GEOTHERMAL STEAM WITH RESPECT TO SILICA SCALING

Direct steam geothermal energy systems for dry steam and superheated steam is described by (DiPippo 2016). Geothermal steam turbines for this commercial application range in size from 10 MW to 120 MW. The smaller units are single flow machines, the mid-range units are double-flow turbines and the larger capacities are either two flow or four-flow machines depending on economic considerations. The capacity of a single flow turbines can be up to 40 MW and the advantage of these is a low profile installation. Single flow turbines make up for about 43% of all geothermal energy plants (DiPippo 2016). The double flash produce excess steam in a second flashing process. It has been shown to be able to produce up to 20-25% more power than a single flash. After recent advances in turbine design, especially qualification of longer Last-stage blades, the optimum capacity of an additional unit or a new geothermal power plant has increased to 80 MW. The optimal turbine capacity for a new system is however affected by total capacity of the field and energy density of the fluid.

(Karlsdottir, Palsson et al. 2010) summarizes a comparison of power output, energy efficiency and economic feasibility for the most common geothermal systems with respect to fluid enthalpy in the range between 1000 kJ/kg to 2500 kJ/kg. The geothermal fluids considered were in the liquid phase and relied on flashing. The comparison includes a standard single flash cycle, conventional double flash cycle, bottoming organic Rankine cycle coupled in parallel to the single flash cycle, using isopentane as a working fluid and lastly, a modification of the double flash cycle with an added recuperator used to superheat the steam at the outlet of the high pressure turbine. For the high enthalpy cases tested (up to 2500 kJ/kg) a double flash cycle was shown to increase power output by 26%. This is lower than the expected enthalpy for the cases considered in the present work where fluid enthalpy at wellhead is approximately 3000 kJ/kg

Before entering the turbine the superheated steam has to be purified. This can be done in a scrubber where the steam is de-superheated by spraying with water through a nozzles in the top. The solids are washed away and mist removed. The steam leaves as saturated steam and the purification essentially represents an undesired energy loss. Residence time and type of washing necessary may vary depending on the steam composition. Scrubbing experiments on IDDP1 showed that silica could be effectively removed with pure water/condensate steam washing, while Sulphur required NaOH for removal (Hauksson, Markusson et al. 2014). Salton Sea geothermal area in southern California has hot dry steam highly contaminated with solids. To purify the steam before injection into the turbine a flash-crystallizer/reactor-clarifier technology and pH modification is applied. In the flash crystallizer, seeds of solids are injected as a slurry into the scrubber providing a large surface for particle growth. The solids are recycled with the separated liquid. The technique has proven effective to reduce growth in the scrubber and downstream equipment (Featherstone, Butler et al. 1995)

The geofluid considered in the present study differs in pressure and chemical composition compared to existing dry steam systems. (Hjartarson, Sævarsdóttir et al. 2013) performed a comparison of system solutions for IDDP1 steam with regard to corrosion. Some experimental investigations of effect of scrubbing methods with the intention of preserving steam superheat was done by (Chauhan, Gudjonsdottir et al. 2019).

3.1 Single stage turbine with no steam purification

Figure 2 gives a schematic overview of a single flash turbine system with a throttling valve. The lines in red mark areas of the process where the fluid will be supersaturated with respect to silica for the hot case. It is assumed that the wellhead fluid has a temperature of 500 °C and 350 bar pressure when entering the system. For the further calculations a mass flow of 50 kg/s is assumed. In reality dynamic conditions will give a significant pressure loss from the reservoir to the wellhead. The well and wellhead pressure will depend on well permeability, hydrostatic and frictional pressure drop. Wellhead pressures of 85 bar is calculated for the IDDP2 well at 30 kg/s production (Sæther 2020). The downhole pressure at 4400 m depth corresponding to this production rate is calculated to 210 bar. For simplicity the frictional pressure loss and temperature loss in the production well is neglected.

Assuming 85% steam quality can be accepted at steam turbine exit, the geothermal fluid must be depressurized along the constant enthalpy curve of 3000 kJ/kg before entering the turbine. The steam is then expanded through the turbine to an exit quality of 0,85. The allowable steam quality at the exit and the minimum condenser operating pressure will decide how much depressurization is necessary to optimize the power output. In the hot case the optimal operating pressure for the turbine inlet is approximately 47 bar when restricting the outlet pressure to 0,1 bar. This is shown as the central black line in Figure 2. According to equation (5) the turbine power output is 38,7 MW. In this equation W is the turbine work output in kJ/s, m is the specific mass flow in kg/s, h_i are the enthalpies at the turbin inlet and outlet. A turbine dry isentropic efficiency of 0,85 is assumed. Generator efficiency is not accounted for in these numbers, but this is normally very high (96%). To account for reduced efficiency of a wet expansion the Baumann rule can be applied. This rules states that a 1% average moisture causes roughly a 1% drop in turbine efficiency. (DiPippo 2016). For this analysis the wet expansion turbine efficiency calculated by equation (6) (Hjartarson, Sævarsdóttir et al. 2013) reduces to 78,6%. In this equation x_{outlet} is the quality at the exit, η_{td} the dry turbine efficiency and η_{tw} the wet turbine efficiency. This may be a conservative approach. Turbine interstage draining reduces power loss due to droplets. For the case evaluated here, the superheat is large and only the part of the expansion occurring beneath saturation will contribute to power loss due to droplet formation. The black solid line in Figure 2 represents the isentropic expansion. The dotted line represents the real expansion. As the outlet conditions is given the optimal pressure reduction is found by calculating the quality and entropy in stage 3s based on the given quality in stage 3, the enthalpies and the wet turbine expansion efficiency. If throttling to a higher pressure the steam quality would be too low at an exit pressure of 0,1 and higher condenser pressure would reduce work output. If throttling to a lower pressure, the quality at the exit would be better than required, but this also reduces overall turbine power output.

$$W_{turbine} = m(h_2 - h_3)\eta_{turbine} \tag{5}$$

$$\eta_{tw} = \frac{\eta_{td}(1 + x_{outlet})}{2} \tag{6}$$

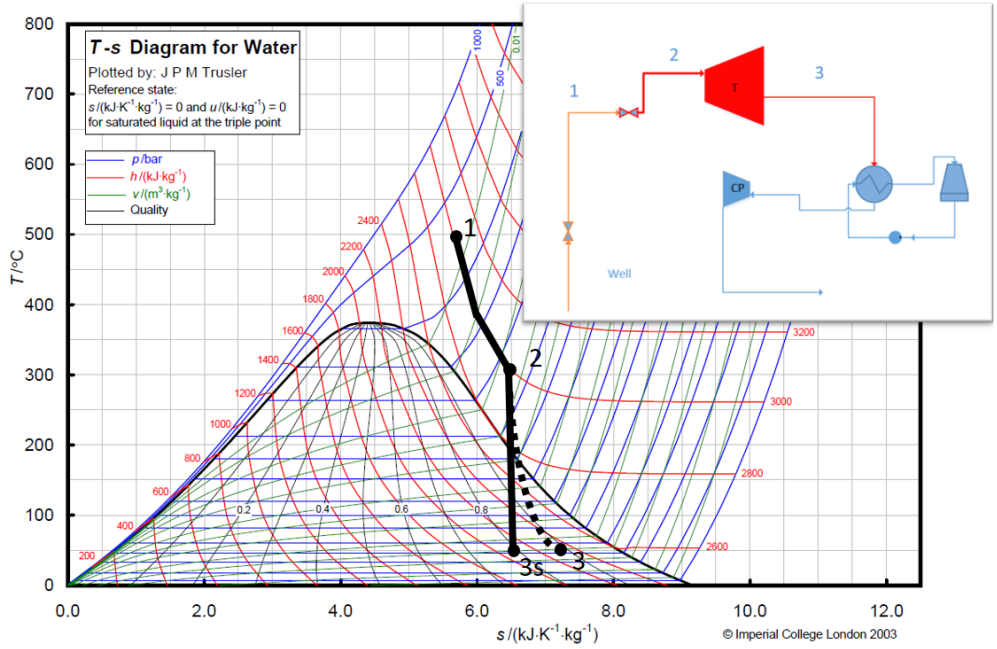

Figure 2 :Single stage turbine system schematic and T-s diagram with segments vulnerable to silica scaling illustrated in red

In the supercritical region the steam does not behave as an ideal gas and pressure reduction at constant enthalpy is associated with a significant temperature loss. In the case of throttling to 75 bar, the temperature will drop 150 ℃ (down to 350 ℃). If throttling to 10 bar, the temperature will drop further, to 275 ℃. Due to the low exit pressure, the used geothermal brine will have to be pumped up to a higher pressure in order to be injected into the reservoir. The pump work for cooling and pressurizing the fluid will reduce the net power output from the system.

Using the steam directly in a conventional steam turbine without pre-purification as sketched out here has several potential issues. The steam contains volatile compounds that will form strong hydrochloric acid upon condensation of the first drops. This may cause pitting corrosion, inner crystalline corrosion and stress corrosion cracking that will degrade the turbine blades in the last stages of the expansion. Some work has been aimed at investigating materials that are resistant to this type of corrosion (Kritzer 2003), (Karlsdottir, Krogh et al. 2019), (Karlsdottir, Ragnarsdottir et al. 2014), (Karlsdottir, Thorbjornsson et al. 2013), (Thorhallsson 2018), (Karlsdottir, Krogh et al. 2019), (Tjelta, Krogh et al. 2019) but utilization without chemical treatment of the geothermal steam before utilization is unrealistic with current day technology.

Another issue is silica scaling. When looking at saturation data for pure water systems and assuming the reservoir fluid is in equilibrium with quartz, the concentrations of silica in the system will be approximately 190 mg/kg (Fournier and Potter 1982b). If interpolating between the experimental data for amorphous silica solubility of (Heitmann 1964) for enthalpy of approximately 3000 kJ/kg as shown in Figure 3, the equilibrium point for amorphous silica will pass 190 mg/kg at 297 bar. Assuming a reservoir pressure of 350 bar, more than 52 bar pressure drop will lead to fluid supersaturation with respect to silica. According to calculations by (Sæther 2020) (Figure 8), geothermal fluid may become supersaturated already between reservoir and borehole. The fluid will further undergo a rapid increase in supersaturation through the well and topside throttling valve. At 28 bar the equilibrium concentration in the steam is approximately 1,2 mg/kg according to the experimental data of (Heitmann 1964), meaning that if no previous precipitation has occurred the fluid will exit the throttling valve with a supersaturation index of over 200.

The very rapid change in supersaturation occurring during a throttling, where the solution goes from undersaturated to highly supersaturated in only seconds, will cause silica to polymerize rapidly into nuclei in the solution and form many relatively small particles. There is, however, great uncertainty regarding the reaction kinetics of amorphous silica in steam. Comparing the measured concentrations of silica in IDDP1 to the equilibrium data available for amorphous silica in pure water and experienced precipitation, suggest that once the super saturation index exceeds 2, silica in the steam will start to polymerize (Marrkússon, Einarsson et al. 2013). As the very high supersaturation facilitates rapid generation of nuclei, less excess silica monomers will be left to cause further growth of particles. Further growth of the 1-5 nm size polymers will therefore be determined by agglomeration. The agglomeration will depend on the solution pH and composition. At low pH and/or with relatively high salt content it is likely that the silica polymers will agglomerate into gel clusters resembling larger porous particles (Iler 1979). The result is a low-density dust like precipitate. Further depressurization in the turbine may create more silica monomers that help facilitate agglomeration by bridging particles.

If precipitated material is already present in the fluid, the increase in supersaturation may result in monomeric deposition onto the existing particles and further cementing of agglomerates. Experience from the Salton Sea plant in California has shown that seed

crystallization, by injection solid material into separatFors is an efficient method for increasing precipitation rates of silica and iron silicate from the liquid water (Featherstone, Butler et al. 1995). Silica precipitate in water is able to form a monodisperse solution if allowed to mature. This is because the solubility is dependent on surface curvature. The smaller particles will dissolve and the larger particles grow on their expense. With the large and rapid increase in supersaturation that follows a throttling process homogenous nucleation will probably take place even with a rather large surface area of seed matter/previously precipitated material available for growth.

The valve itself, piping and all equipment downstream of the throttling valve will be exposed to the precipitate as illustrated with the red lines in Figure 2. This porous material is easy to remove by water jetting and may not cause mechanical difficulties when operating the valves, but the valve sealing mechanism and materials must be chosen carefully to avoid problems. If deposits cannot be flushed out during operation, the volume and growth rate of deposits is expected to affect regularity. Severe scaling inside the turbine must also be expected for this case. More research is required to determine the behavior of a silica particle in high velocity flow across curved surfaces like in a turbine to determine depositional rates. Also the microstructure and physical properties of the resulting deposit needs to be examined to determine the maintenance requirements.

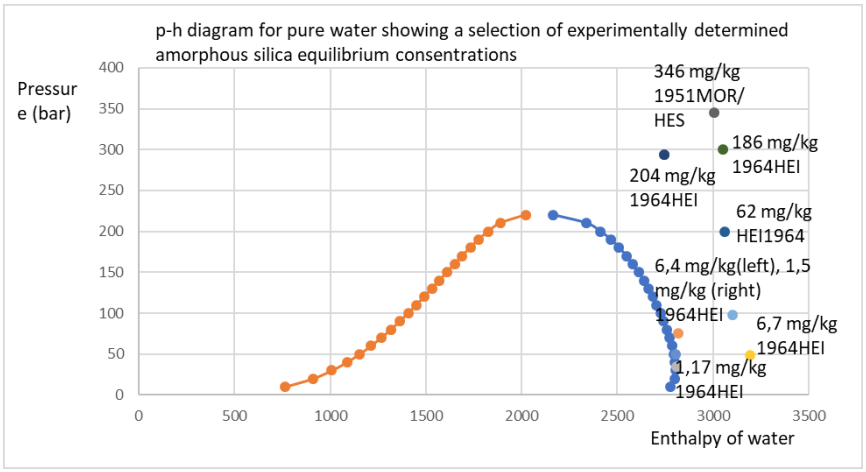

Figure 3: Some experimental data for amorphous silica equilibrium concentrations in pure water (Plyasunov 2011), (Heitmann 1964), (Morey and Hesselgesser 1951)

At 10 bar the fluid will have entered the two-phase region and the equilibrium concentration of amorphous silica in the steam phase can be expected to be around 1 mg/kg. Assuming no previous precipitation the super saturation can be very high. If precipitation occur instantaneously, the supersaturation may remain through the turbine as the pressure reduction through the turbine will reduce equilibrium concentration in the steam further. It is interesting to note that at the turbine exit, where 15% liquid water is present, this liquid water will be undersaturated with respect to silica, as the equilibrium concentrations on the liquid side of the phase diagram is much higher. When exiting the turbine at 0.1 bar, the temperature of the liquid will be approximately 45 °C, which gives an amorphous silica equilibrium concentration of approximately 250 mg/kg. In the case of 50kg/s water and 190 mg/kg silica, where the amount of water is 7,5 kg/s and the amount of steam 40,25 kg/s, the total amount of silica is 9,5 g/s. If the mixing is perfect the silica will be distributed unevenly so that more is dissolved into silicic acid in the liquid and the supersaturation in the remaining steam decrease. Total equilibrium concentration has gone from 1 mg/kg to 36 mg/kg. If all excess silica has precipitated dissolution may occur, but this is expected to have a longer induction time than the precipitation process.

Several solutions for purification of the steam is available, but most of these will reduce power output from the system. (Hjartarson, Sævarsdóttir et al. 2013) compared several techniques for mitigating corrosion from the chloride bearing steam. Scrubbing is one of the alternatives that has proven efficient for both neutralizing the hydrochloric acid (by injection of NaOH) and also for silica removal (Hauksson, Markusson et al. 2014). From the alternatives discussed by (Hjartarson, Sævarsdóttir et al. 2013), Dry scrubbing contributed to very little power loss. Only 0,5 MW compared to the direct dry steam simulation (1,2 % reduction). The single flash with scrubbing had a 14% lower power output than the single flash dry steam solution. In a dry scrubbing system the steam does not need to be cooled. Solid or liquid material is either injected into the stream or absorbed in a reactor vessel (D.W. Fisher 1996) (Hirtz, Broaddus et al. 2002). When the chemicals have mixed with the flow, it is driven through some sort of a separator, such as an electrostatic precipitator or a bag house filter, where the injected material is filtered out, along with the adsorbed or absorbed contaminants. For the material already precipitated dry scrubbing may prove efficient for silica removal if placed after the throttling valve. At pH above 2 the silica surface will have a negative charge and should respond to a surface with opposite charge. The surface charge of silica particles will be affected by degree of hydration, porosity and other constituents in the steam that may either form surface complexes that increase or decrease the charge, or orient themselves at the surface, cancelling out the particle surface charge. In a dry scrubber where the chemical composition of the fluid is known, the surface charge can be manipulated by additives. Further research is required to prove dry scrubbing efficient for silica particle removal from supercritical steam. It is also required to have more data on the kinetics and polymer behavior of the silica directly after precipitation.

3.2 Single stage turbine with scrubbing

The single flash cycle where the steam is scrubbed is depicted in Figure 4. The optimal scrubber and turbine entry pressure is lowered to 11 bar. The scrubbing process involves removing some of the superheat, quenching the steam by droplets of condensate and chemicals inserted through nozzles in the top. If adhering to the exit limitations of the previous example and assuming that the steam will have to be quenched (point 2-3 in Figure 4). The expansion gives significantly less power output. A total of 29,8 MW is estimated

for the optimal throttling pressure of 11 bar. This is 23 % less than without scrubbing. To ensure sufficient scrubbing, it is assumed that the mass flow of silica enriched water leaving the scrubber is 2% of the steam flow at exit. An energy balance and mass balance over the scrubber gives the necessary condensate injected and the saturated steam mass flow out of the scrubber. An injection stream of 4,9 kg/s pure water with temperature 20 °C and pressure of 11 bar is calculated by equation (7) and (8). The enthalpy lost from the superheated steam vaporizes the liquid droplets injected and 53,7 kg/s saturated steam exit the scrubber in stage 3.

$$m_2 h_2 + m' h' = m_3 h_3 + m_{liquid} h_{liquid} \tag{7}$$

$$m' + m_2 = m_3 + (1 - 0,98) m_3 \tag{8}$$

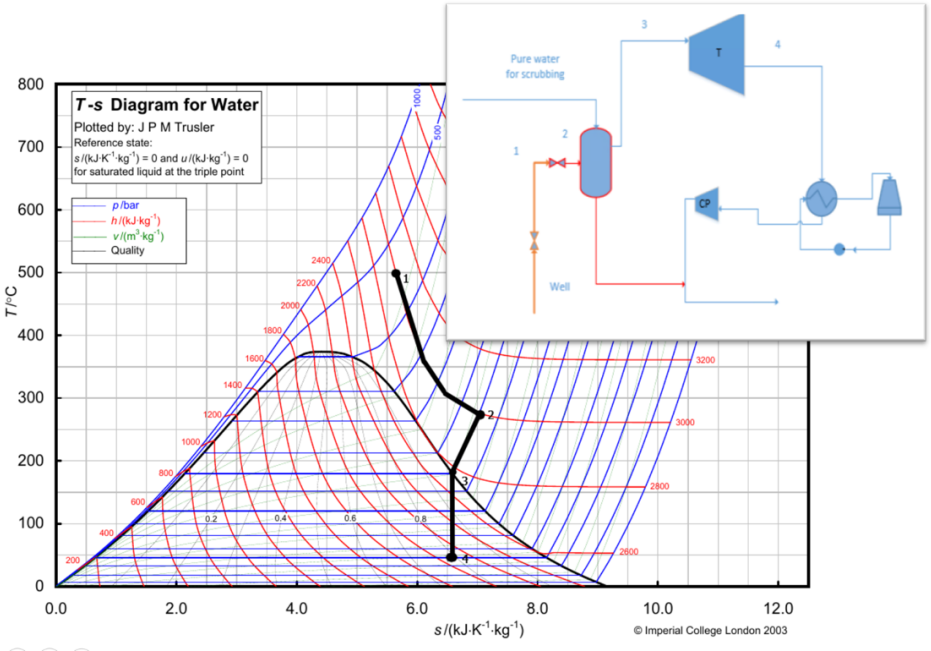

Figure 4: Schematic and T-s diagram of single flash turbine system with scrubbing with segments vulnerable to silica scaling illustrated in orange and red

The liquid drops injected to the scrubber by nozzles effectively removes solids from the steam, and the hydrochloric components in the steam can be neutralized to avoid corrosion in the turbine. As shown in Figure 4, the throttling valve and the piping between the valve and the scrubber will be exposed to steam highly supersaturated with silica. Bends and straight pipes downstream of the throttling valve will probably experience clogging. The inner part of bend outlets will potentially have the highest depositional velocities (Karlsdottir, Ragnarsdottir et al. 2014). Problems can be avoided by placing the throttling device close to the scrubber and by having a system for valve flushing.

If 1kg/s water exit the scrubber for each 50 kg/s of steam that enters the scrubber, the concentration of silica in the liquid will be approximately 12,5 g/s. At a temperature of 180 °C approximately 800-900 mg/kg can dissolve in the liquid if allowed time to do so, still most of the silica will remain in solid form. Silica must be removed before reinjection to avoid clogging the injection well. Scaling in the scrubber itself and downstream the scrubber may reduce regularity. Both seed crystallization, pH modification and maturation techniques has proven effective to avoid silica and iron silicate on geothermal processing equipment (Villaseñor and Calibugan 2011) (Borrmann and Johnston 2017) (Gudmundson and Einarsson 1989).

3.3 Two turbine solutions

In the solution sketched out in Figure 5, the supercritical steam is utilized by directly running the geofluid first through a backpressure turbine (1-2). Due to the corrosiveness of droplets formed upon the first condensation of unpurified steam, there must be a safety limit ensuring that the steam stays above saturation line on the last stages of the turbine. With a 10% margin (thermodynamic quality of 1,1), the superheated steam exit the turbine with an enthalpy of 2830 kJ/kg at a pressure of 100 bar. The enthalpy is utilized to generate 8,5 MW power by the back pressure turbine.

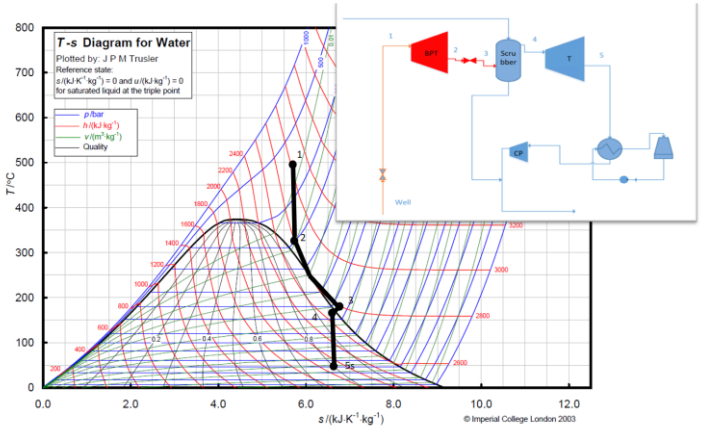

Figure 5: Schematic representation and T-s diagram of a two-turbine system with dry first stage expansion and scrubbing between high pressure and low-pressure turbine. Red and orange line mark areas vulnerable to silica scaling

The steam is purified in a scrubber before it can enter the low-pressure turbine. The superheated steam is depressurized along the constant enthalpy line of 2830. The superheated steam is very close to saturation at pressures between 20 and 50 bar, so the valve may be exposed to corrosive droplets. In step 3-4 it is assumed that the steam is quenched. Mass and energy balance (equation (7) and (8)) give injected pure water of 1,7 kg/s and mass flow out of the scrubber of 50,6 kg/s. The cooling and corresponding exergy loss due in stage 3-4 is less than was the case for the single turbine with scrubbing. The purified steam is further utilized in a conventional low-pressure turbine. As previously, the pressure is reduced to 0,1 bar and exits the low pressure turbine with a steam quality of 0,85. The power output from the low pressure steam turbine is estimated to 28,1 MW and the total power output from the two turbines is approximately 36,6 MW. A two turbine solution is more expensive and the 8,5 MW generated by the back pressure turbine must justify the cost of an extra turbine.

As illustrated in Figure 5 the backpressure turbine is considered to be vulnerable to silica deposition. Due to frictional pressure losses, the geofluid may already be slightly supersaturated when entering the turbine. Through the expansion equilibrium concentration reduces to approximately 16 mg/kg, which gives a supersaturation index of 11 assuming no previous precipitation has taken place. The particles formed may be larger than after the throttling valve due to the gradual increase in supersaturation, as opposed to the sudden increase experienced in the throttling valve. Further research is required to determine if a turbine design can handle these amounts of solids, but it is likely that solidified silica can lead to erosion, degrading turbine performance due to scaling on turbine blades and clogging, posing significant regularity and performance issues. A design robust with regard to scaling, like a screw expander may be more suited. The volume ratios associated with a pressure drop from 350 to 100 bar are higher than conventional screw expanders are normally designed for.

For comparison, Figure 6 shows a two turbine solution with separation and scrubbing between the turbines where minimum steam quality at both turbine exits are 0.85%. The geofluid enters the top turbine at stage 1, and leaves at stage 2. The fluid is then separated and since the quality is already 0,856 in the flash tank it is assumed that mass addition for purification is not required. The steam exiting the flash tank is further expanded to a quality of 85% and a pressure of 0,1 bar as previously. In this case the total power output can be as high as 48,9 MW (25,1 MW from the high-pressure turbine and 23,8 MW from the low-pressure turbine). This is 25% higher than if exiting the high pressure turbine with thermodynamic quality of 1,1 as previously discussed. However, there is no scale or corrosion mitigation in the high-pressure turbine exposed to both highly corrosive hydrochloric acid and to a very high solids content leading to scaling. Robust operation of a turbine exposed to these conditions represents a technology gap. A two-turbine solution with steam purification in between provides 23% higher power output than the single stage turbine with no purification. If several wells are connected on one turbine system and thus increasing the mass flow and power output, a double turbine system may be justified.

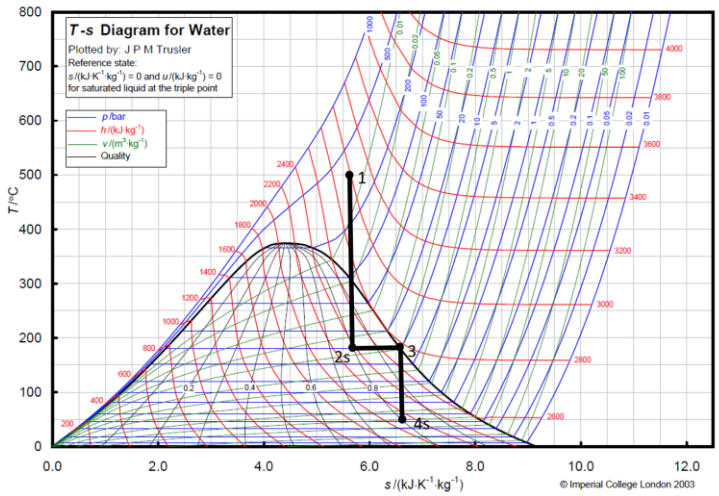

Figure 6: T-s diagram for a two-turbine configuration with no purification on the first step

3.4 Reheat options

3.4.1 Reheat option 1

In the first option, sketched out Figure 7, the total mass flow of supercritical geothermal steam is used to reheat the saturated steam after scrubbing. Some of the heat loss necessary to perform an efficient scrubbing is recovered. Pressure drop in the heat exchanger is not accounted for and heat exchanger size requirements are not calculated in this analysis. Energy conservation for the heat exchanger, equation (9), gives the rate of enthalpy change for the two streams. The geofluid is cooled to approximately 473 °C and throttled along the 2850 kJ/kg enthalpy line to 35 bar. Only 1,65 kg/s scrubbing water is added in this example. The saturated steam leaving the scrubber is reheated to 289 °C. The power output is calculated to 36,6 MW according to equation (5). With the given assumptions, this solution gives a power increase of approximately 20% when compared to the single turbine with scrubbing. The power output can be increased further if further cooling and throttling of the two-phase region is allowed for (40 MW if cooled to an enthalpy of 2700 kJ/kg).

$$m(h_1 - h_2) = m(h_5 - h_4) \tag{9}$$

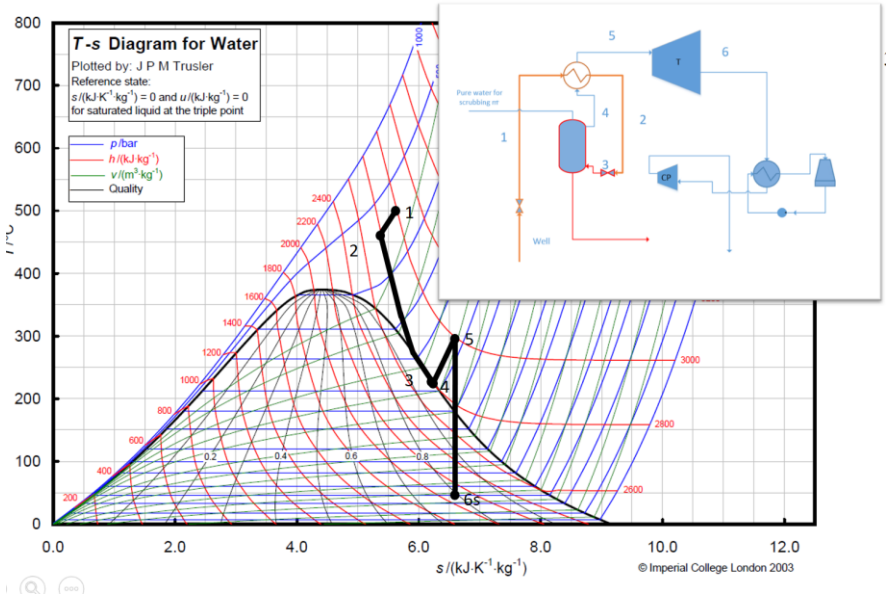

Figure 7: Simplified schematic and T-s of a solution with reheat of the saturated steam from the scrubber by heat exchanging with the superheated geofluid at full pressure

Although a potential power increase of 20% is significant, a rather large and costly heat exchanger is required in this case. The volumetric flow on the low pressure side is 3,4 m^3/s. There may be cost optimizations on the pressure in stage 4. The high pressures of the supercritical fluid combined with the high temperature sets unconventional requirements to the piping spec. Corrosion control in supercritical steam at low pH and a potentially hazardous composition is not fully understood, and material selection requirements will be important.

The heat exchanger will also be exposed to scaling, but the equilibrium concentration of amorphous silica will increase inside the heat exchanger giving a decrease in supersaturation. The scaling potential is therefore determined by previously precipitated material. A rough scale layer may increase turbulence in the pipes and thereby increase heat transfer, but pressure drop will decrease overall performance over time. Increased roughness also greatly increases deposition rates (Guha 2008). Because the particles are small, with relaxation times below 0,1, temperature difference between the pipe wall and the bulk fluid will also cause increased mass transfer due to thermophoresis. (Guha 2008) showed that a temperature difference of only 20 K might increase the depositional rates by a factor of 100.

3.4.2 Reheat option 2

In Figure 8, a small amount of the superheated geofluid is used to reheat the saturated steam after the scrubber. In this solution the distribution of mass between the turbine and the reheater and the turbine inlet pressure is optimized to get the maximum power output from the second turbine. The energy balance for the heat exchanger is given by equation (9). Assuming that the heat exchanger pinch point is 5 K, the temperature at stage five is given by $T_5=T_2$-5K.

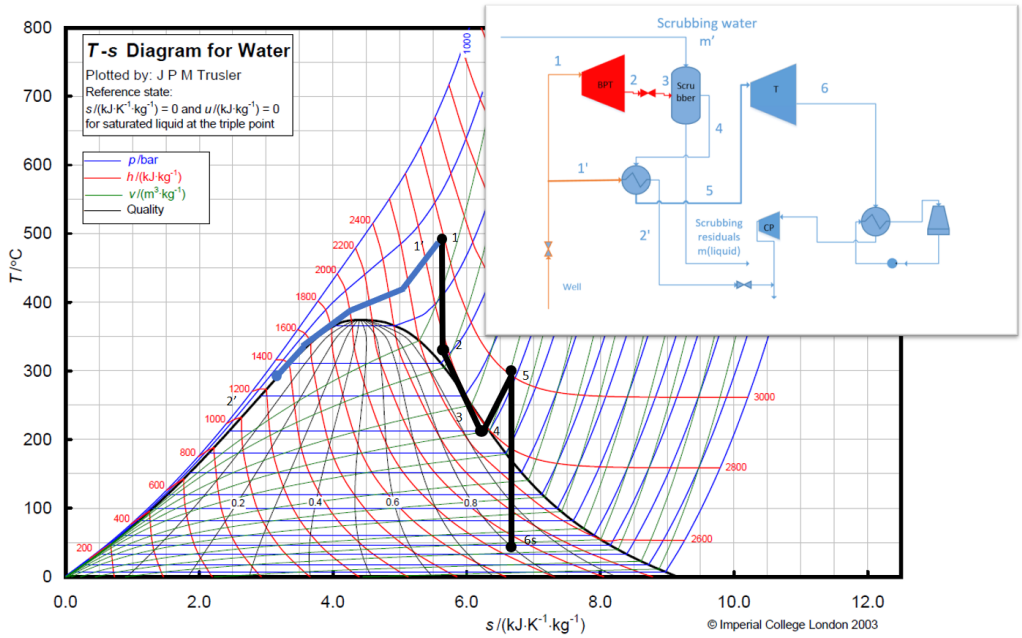

Figure 8: Schematic and T-s diagram for reheat option 2.1. Dry first expansion where part of geofluid is used to reheat the main stream before entering the low-pressure turbine

In this example, using 6% of the mass flow for reheating the geothermal fluid gives a power output of 39,5 MW total. This is 7% higher than the comparable backpressure turbine case with no reheat. The backpressure turbine is as exposed to scaling as discussed previously. The heat exchanger will also be directly exposed to geothermal fluid and will be operating close to saturation line.

The fluid used for reheat has an enthalpy of 1212 kJ/kg when exiting the heat exchanger in step 2'. The remaining heat in the pressurized liquid water can be utilized by throttling down to 29 bar and reinjection the two-phase mixture into the scrubber as shown in Figure 9. The quality of stream 3' at 29 bar would be 0,21 and the increase in power output 0,5%.

Reheat case 2.1 assumed a thermodynamic quality of 1,1 at the exit of the first turbine. Comparing with the case where the exit quality in stage 2 is 0,86 at 12 bar pressure as shown in Figure 9, the power output is higher. This cycle uses 0,3% of the mass for reheat and the power output is 49 MW, approximately the same as two wet expansions without reheat. Increasing the exit pressure after the first turbine decreases power output.

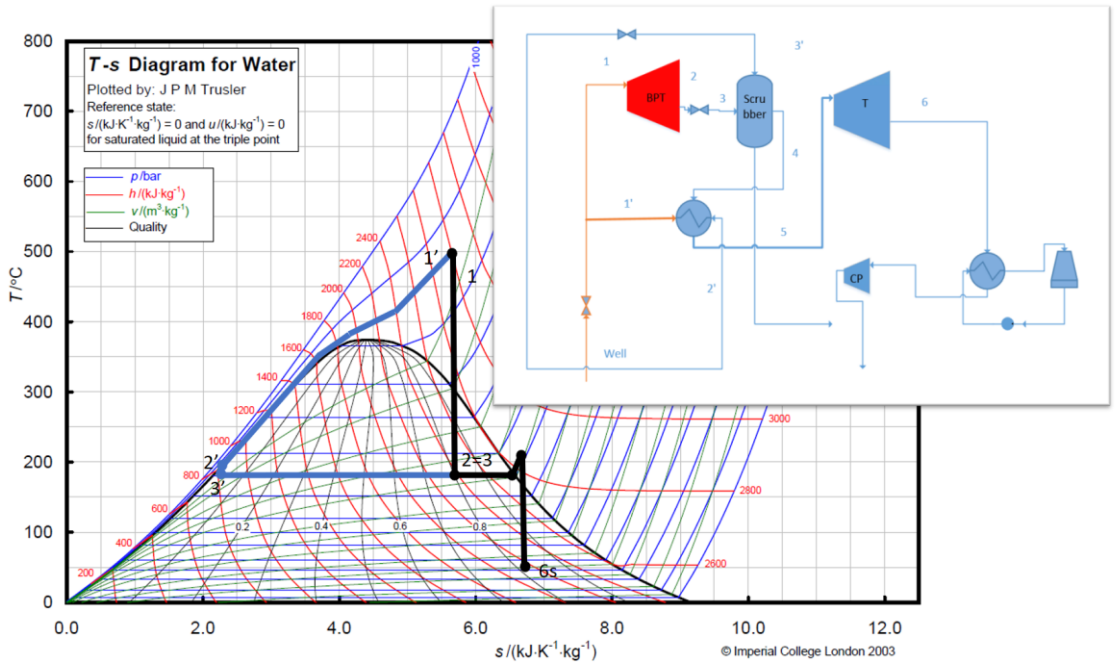

Figure 9 :Simplified schematic and T-s diagram of reheat option 2.2. Two wet expansions where part of geofluid is used to reheat the main stream before entering the low pressure turbine. Fluid used for reheat is reinjected into the scrubber.

3.5 Binary top cycle with single flash bottom

In the case illustrated in Figure 10, all of the superheated geothermal fluid is utilized directly in a heat exchanger where enthalpy is transferred to a secondary medium that may be pure water or mineral lean condensate. For this analysis it is assumed that the secondary medium is liquid condensate from the flash separator/scrubber. The hot water leaving the scrubber is reused, increasing overall energy utilization. The fluid is separated in stage 5 and then purified. In the purification process mass is added for the second cycle. In the calculation example approximately 1,6 kg/s of pure water at 20 °C was added to the mass flow. The heat required for the added mass is accounted for by assuming ambient inlet conditions. So is pump work from separation pressure to optimal pressure for turbine entry. Otherwise it is assumed that energy is preserved so that the liquid leaves the purifier at saturation temperature for 11 bar and is pumped to optimal pressure in (1'-2'). The water is heated in three stages. A preheater, a boiler and a superheater. The mass flow in the second cycle, and thus the available superheat is given by the enthalpy in stage 2. The higher the enthalpy at stage 2', the higher quality in the separator and thus, less mass flow and more superheat for stage 4'-5'.

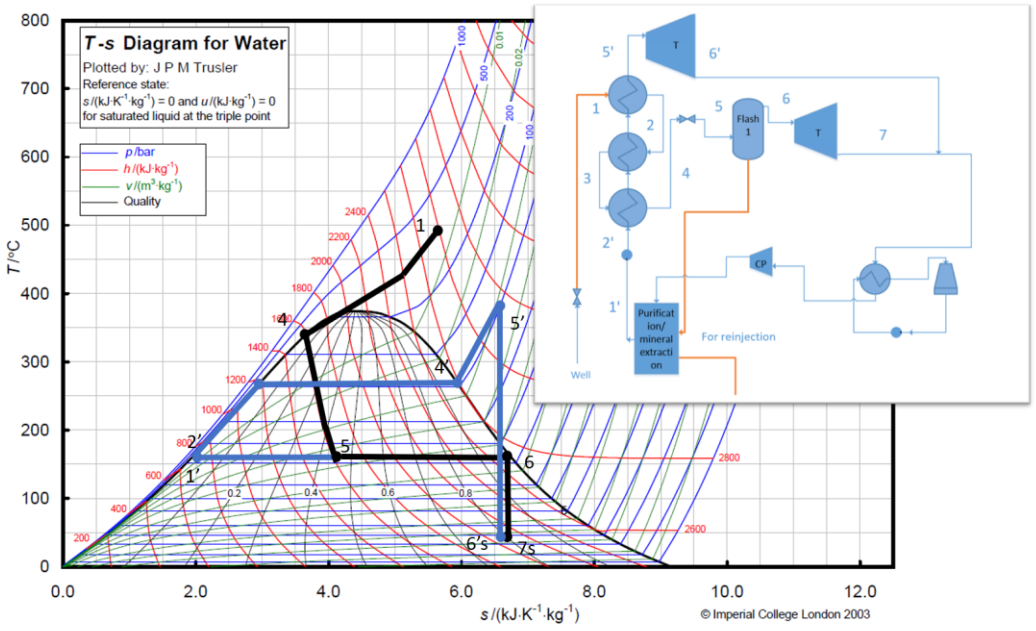

Figure 10: Schematic and T-s diagram of a top binary system with single flash

Energy balance over the heat exchangers (equation (9), with the same assumptions as previously gives an optimal pressure of 62 bar for the second cycle. A total power output of 35,4 MW is estimated. This is 30% higher than for single turbine with scrubbing.

Along the 1-4 line amorphous silica equilibrium concentration is expected to increase. The heat exchanger is thus exposed only to particles already present in the fluid. The density at 350°C has increased from 144 kg/m^3 to 658kg/m^3. The water structure becomes increasingly more liquid like and thus a better solvent for silica. The solution becomes increasingly undersaturated through the heat exchanger and silica scaling should not be a problem unless previously precipitated material is present. The geofluid is then throttled to 7 bar along the constant enthalpy line. The valve may be exposed to corrosion as the fluid enters the two-phase region. Water and steam is separated and steam can be run directly into a steam turbine. At 11 bar the silica equilibrium concentration in the steam is close to 1. Most of the remaining silica concentration will therefore remain in the liquid. If 50% mass is converted to steam the concentration in the remaining liquid will be doubled. A silica concentration of 400 mg/kg water is below equilibrium concentration of liquid water in this situation.

The solution utilizes commercially available turbine systems and few problems caused by silica precipitation are anticipated. The purification method must, however, be evaluated more carefully. If the wellhead pressure is lower than critical pressure, the geothermal fluid in the heat exchanger may become two-phase during the cooling process. If the chemical composition of the geothermal fluid increases the critical point, the fluid may even be two phase upon entry (Bischoff and Rosenbauer 1988). The heat exchanger capacity requirements is also rather large. The geothermal steam will enter the heat exchanger with a volumetric flow rate of 0.35 m^3/s and the superheated purified steam will exit the heat exchanger and enter the turbine with a volumetric flow rate of approximately 1,2 m^3/s.

4. RESULTS

Table 0-1 gives a summary of the cases where maximum power output and the risk of silica scaling is evaluated by risk analysis methodology for each case with the given assumptions. The likelihood of silica scaling is given a score between 1 and 3 based on the calculated super saturation index and the areas affected. The consequence is also given a score between 1 and 3 based on the type of equipment affected, the anticipated severity of process disruption and possibility of maintenance and mitigation. The product of these two give an overall silica scaling risk. The cases are ranked by specific work output times ten over scaling risk.

Table 0-1: Summary of power output and silica scaling risk

Case	Turbine work output (MW per 50 kg/s flow)	Specific net work output (kW/kg/s)	Utilization efficiency comparison	Scaling likelihood	Scaling severity	Scaling risk	Solution ranking
Single turbine with throttling (28 bar)	38,7	751,1	0,535	3	3	9	0,023
Single turbine with scrubbing	29,9	579,2	0,413	2	1	2	0,815
Double turbine with dry first expansion	36,6	710,3	0,506	3	3	9	0,222
Double turbine with two wet expansions	49,0	949,7	0,677	3	3	9	0,297
Reheat Option 1- all of geofluid used for reheat	36,7	711,0	0,507	2	1	2	1,000
Reheat Option 2.1- 6% of geofluid used for reheat in a double turbine solution with dry first expansion	39,5	767,1	0,546	3	2	6	0,360
Reheat option 2.2- small % of geofluid used to reheat in a double turbine solution with two wet expansions	49,0	950,3	0,677	3	3	9	0,297
Top binary cycle with spent fluid reuse	35,4	687,1	0,490	2	1	2	0,966

For the net specific work output a factor of 0,97 is used to account for pump work, cooling and generator efficiency. Utilization efficiency is calculated by equation (10) and (11), where the reference state is 10°C and 1 bar. e is exergy, s entropy, h enthalpy and w_t is the net system work output per unit mass.

$$e = h_1 - h_0 - (T_0 + 273{,}15)(s_1 - s_0) \tag{10}$$

$$\eta_u = \frac{w_t}{e} \tag{11}$$

5. CONCLUSIONS

The power output from a supercritical, high enthalpy geothermal well can be high compared to conventional wells. The power output comparison show that there are significant differences in utilization efficiency for the solution chosen and that there are great challenges with regard to silica scaling for the solutions with the highest power output. Further optimizations and component performance analysis are possible to increase overall power output. The safest commercially available solution with regard to scale prevention in the power system is scrubbing the steam before entering a turbine or a heat exchanger. Reheat option 1 and the top binary cycle however use a heat exchanger where silica supersaturation is expected to drop due to increase in equilibrium value along the isobar. Both these solution can be combined with potassium carbonate scrubbing before the heat exchanger that removes solids

without reducing superheat. This methodology has shown promising results for scrubbing superheated steam (Chauhan 2019), but efficiency has yet to be investigated for the pressures discussed in this paper. The risk of scaling in the wellbore and in the throttling valve is not eliminated in any of the solutions. Scrubbing the steam is 45% percent less efficient than using the steam directly in a two-turbine system with reheat. A complete evaluation, where the solutions are further optimized and where economic considerations, both capital cost and operational costs due to maintenance are considered, will give a clearer picture of the potential in the different solutions

More research is required to determine the properties and behavior of silica particles generated from supercritical geothermal steam. This will give data that can be used to determine more accurately where the silica deposition will occur in specific process system designs. Investigation of the properties of the scale as a function of the particle formation process and depositional mechanism can give valuable information about maintenance strategies for minimum system shutdown.

REFERENCES

Allison, S. (2004). "Analysis of the electrophoretic mobility and viscosity of dilute Ludox solutions in terms of a spherical gel layer model." Journal of Colloid and Interface Science Volume 277 (Issue 1): Pages 248-254.

Bahadori, A. and H. B. Vuthaluru (2009). "Prediction of silica carry-over and solubility in steam of boilers using a simple correlation." Applied Thermal engineering Volume 30(Issues 2–3, February 2010): Pages 250-253.

Bischoff, J. L. and R. J. Rosenbauer (1988). "Liquid-vapor relations in the critical region of the system NaCl-H2O from 380 to 415°C: A refined determination of the critical point and two-phase boundary of seawater." Geochimica et Cosmochimica Acta Volume 52(Issue 8): Pages 2121-2126.

Borrmann, T. and J. H. Johnston (2017). "Transforming Silica into Silicate – Pilot Scale Removal of Problematic Silica from Geothermal Brine." Geothermal Resources Council Transactions Vol. 41: Pages 1322-1333.

Brady, E. L. (1953). "Chemical nature of silica carried by steam." J. Phys. Chem. Vol. 57(7): Pages 706-710.

Brinker, C. and G. Scherer (2013). The Physics and Chemistry of Sol-Gel Processing, Academic Press.

Brown, K. (2011). Thermodynamics and kinetics of silica scaling. Proceedings International Workshop on Mineral Scaling, Manila, Philippines, 25-27 May 2011.

Brown, K. and M. Dunstall (2000). Silica scaling under controlled hydrodynamic conditions. World Geothermal Congress, Kyshu-Tohuku, Japan.

Brunner, G. (2014). Hydrothermal and Supercritical Water Processes, Elsevier.

Chauhan, V. (2019). Superheated Steam Scrubbing and Utilization for Power Generation. PhD, Reykjavik university.

Chauhan, V., M. Gudjonsdottir and G. Saevarsdottir (2018). Silica deposition in superheated geothermal systems. 43rd Workshop on Geothermal Reservoir Engineering, Stanford University, Stanford, California, February 12-14, 2018.

Chauhan, V., M. Gudjonsdottir and G. Saevarsdottir (2019). "Silica scrubbing from superheated steam using aqueous potassium carbonate solution: An experimental investigation." Geothermics Volume 80, July 2019: Pages 1-7.

Churakov, S. (2001). Physical-chemical properties of complex natural fluids. phd, der Technischen Universität Berlin.

D.W. Fisher, D. B. J. (1996). Alternatives to traditional water washing used to remove impurities in superheated geothermal steam. Geothermal Resources Council Transactions, Portland, OR (United States), 29 Sep - 2 Oct 1996.

DiPippo, R. (2016). Geothermal Power Generation- Developments and Innovation, Woodhead Publishing.

Featherstone, J., S. Butler and E. Bonham (1995). Comparison of crystallizer reactor clarifier and pH mod process at the salton sea geothermal field. World Geothermal Conference Florence, Italy: 2391-2396.

Fournier, R. O. and R. W. Potter (1982a). "A revised and expanded silica (quartz) geothermometer."

Fournier, R. O. and R. W. Potter (1982b). "An equation correlating the solubility of quartz in water from 25” to 900°C at pressures up to 10,000 bars." Geochimica et Cosmochimica Acta Volume 46(Issue 10,): Pages 1969-1973.

Fournier, R. O. and J. J. Rowe (1977). "The solubility of amorphous silica in water at high temperatures and high pressures." American Mineralogist Volume 62: Pages 1052-1056.

Gudmundson, S. R. and E. Einarsson (1989). "Controlled silica precipitation in geothermal brine at the Reykjanes geo-chemical plant " Geothermics Volume 18(Issues 1–2): Pages 105-112.

Guha, A. (2008). "Transport and Deposition of Particles in Turbulent and Laminar Flow." Annual Review of Fluid Mechanics Vol. 40: Pages 311-334.

Hack, A. C., A. B. Thompson and M. Aerts (2007). "Phase Relations Involving Hydrous Silicate Melts, Aqueous Fluids, and Minerals." Mineralogy & Geochemistry Volume 65(1): Pages 129-185.

Hauksson, T., S. Markusson, K. Einarsson, S. N. Karlsdóttir, Á. Einarssond, A. Möllere and Þ. Sigmarsson (2014). "Pilot testing of handling the fluids from the IDDP-1 exploratory geothermal well, Krafla, N.E. Iceland." Geothermics Vol. 48: Pages 76-82.

Heitmann, H. G. (1964). Die Loslichkeit von Kieselsaure in Wasser und Wasserdampf sowie ihr Einfluss auf Turbinenverkieselungen. PhD, Technische Hochschule Karlsruhe.

Hirtz, P. N., M. Broaddus and D. Gallup (2002). "Dry Steam Scrubbing for Impurity Removal from Superheated Geothermal Steam." Transactions - Geothermal Resources Council Vol. 26.

Hjartarson, S., G. Sævarsdóttir, K. Ingason, B. Pálsson, W. S.Harvey and H. Pálssone (2013). "Utilization of the chloride bearing, superheated steam from IDDP-1." Geothermics Volume 49: Pages 83-89.

Iler, R. K. (1979). Chemistry of silica- Solubility, Polymerization, Colloid and Surface Properties and Biochemistry, John Wiley & Sons.

J. Nestor, J. E. (2016). Silica and Titania Nanodispersions (Chapter 5). Nanocolloids- A Meeting Point for Scientists and Technologists: 536.

Jacobson, N. S., E. J. Opila, D. L. Myers and E. H. Copland (2005). "Thermodynamics of gas species in the Si-O-H system " The Journal of Chemical Thermodynamics Volume 37(Issue 10, October 2005): Pages 1130-1137.

Karásek, P., L. Šťavíková, J. Planeta, B. Hohnová and M. Roth (2013). "Solubility of fused silica in sub- and supercritical water: Estimation from a thermodynamic model." The Journal of Supercritical Fluids Volume 83: Pages 72-77.

Karlsdottir, M. R., H. Palsson and O. P. Palsson (2010). Comparison of Methods for Utilization of Geothermal Brine for Power Production World Geothermal Congress 2010, Bali, Indonesia.

Karlsdottir, S. N., B. C. Krogh, S. Sæther and G. Þórólfsson (2019). Corrosion damage of injection string from the deep geothermal well IDDP-2 in Reykjanes Iceland. NACE international. Nashville, Tennessee, USA.

Karlsdottir, S. N., K. R. Ragnarsdottir, A. Moller, I. O. Thorbjornsson and A. Einarsson (2014). "On-site erosion–corrosion testing in superheated geothermal steam." Geothermics Volume 51: Pages 170-181.

Karlsdottir, S. N., I. O. Thorbjornsson and T. Sigmarsson (2013). Corrosion and Scaling in Wet Scrubbing Equipment of Superheated Geothermal Well IDDP-1 in Iceland NACE.

Kennedy, G. C. (1944). "A portion of the system silica–water." Economic Geology Vol. 45: Pages 629-653.

Kokhanenko, P. (2014). Hydrodynamics and Chemistry of Silica scale formation in Hydrogeothermal systems. phd PhD, University of Canterbury, Christchurch, New Zealand.

Kritzer, P. (2003). "Corrosion in high-temperature and supercritical water and aqueous solutions: a review." The journal of supercritical fluids Volume 29(Issues 1–2): Pages 1-29.

Lewis, A., M. Seckler, H. Kramer and G. v. Rosmalen (2015). Industrial Crystallization, Fundamentals and Applications

Marrkússon, S., K. Einarsson, B. Pálsson and Landsvirkjun (2013). IDDP 1, Flow test 2010-2012, LV-2013-050. Landsvirkjun, Landsvirkjun: 341.

Masanori, Toshiya M., S. Yoichi Shimoike and Kenji Notsu (2014). "High SiF4/HF ratio detected in Satsuma-Iwojima volcano's plume by remote FT-IR observation." Earth, Planets and Space Volume 54(Issue 3): Pages 249–256.

Morey, G. W. and J. M. Hesselgesser (1951). "The solubility of some minerals in superheated steam at high pressures." Economic Geology Vol 46 (Issue 8): Pages 821-835.

Palmer, D. A., R. Fernández-Prini and A. H. Harvey (2004). Aqueous Systems at Elevated Temperatures and Pressures- Physical Chemistry in Water, Steam and Hydrothermal Solutions, Academic Press.

Papirer, E. (2000). Adsorption on Silica Surfaces, CRC Press.

Plyasunov, A. V. (2011). "Thermodynamic properties of H4SiO4 in the ideal gas state as evaluated from experimental data." Geochim. Cosmochim. Acta.

Plyasunov, A. V. (2012). "Thermodynamics of Si(OH)4 in the vapor phase of water: Henry's and vapor– liquid distribution constants, fugacity and cross virial coefficients." Geochimica et Cosmochimica Acta Volume 77: Pages 215-231.

Smoluchowski, M. (19117). "Drei Vorträge über Diffusion, Brownsche Molekularbewegung und Koagulation von Kolloidteilchen."

Sæther, S. (2020). Estimating Flow Performance of IDDP-2/DEEPEGS Well by Introducing Local Injectivity Indexes for Different Reservoir Depths. World Geothermal Congress 2020, Reykjavik, Iceland.

Thorhallsson, A. I. (2018). Corrosion Testing of UNS N06625 in a Simulated High Temperature Geothermal Environment. NACE international. Phoenix, Arizona, USA, NACE international.

Tjelta, M., B. C. Krogh, S. Sæther and M. Seiersten (2019). Corrosion, Scaling and Material Selection in Deep Geothermal Wells – Application to IDDP-2. NACE international- Corrosion 2019. Nashville, Tennessee, USA, NACE international.

Villaseñor, L. B. and A. A. Calibugan (2011). Silica Scaling in Tiwi – Current Solutions. Proceedings International Workshop on Mineral Scaling 2011, Manila, Philippines.

Zarrouka, S. J., B. C. Woodhursta and C. Morris (2014). "Silica scaling in geothermal heat exchangers and its impact on pressure drop and performance: Wairakei binary plant, New Zealand." Geothermics Volume 51: Pages 445-459.